Equivalent fire resistance of composite slab made with lightweight concrete

A Lakhal, A Bougara, N Benlakehal

This study examines the fire behaviour of composite slabs made with lightweight concrete, following the fire insulation criteria "I" outlined in Eurocode 4 (CEN 2005). The parametric analysis includes the effect of the airgap, moisture content, thermal properties of the lightweight concrete, and geometrical aspects. Fire resistance time is calculated using two methods – the analytical method from Appendix D of Eurocode 4 (CEN 2005) and a numerical method (ANSYS n.d.). Finite element analysis shows that the moisture content of lightweight concrete significantly impacts fire resistance time. When the moisture content exceeds 3%, the Eurocode method predicts a lower fire resistance time compared to the simulation method. The prediction models indicate that, to achieve the same fire resistance time, a normal-weight concrete section must be 7% thicker than a lightweight concrete section.

Keywords: composite slab, lightweight concrete, fire resistance, moisture content, numerical simulation.

INTRODUCTION

Horizontal elements known as composite slabs are formed by casting concrete over profiled steel sheeting, which functions as a permanent formwork and provides a safe working platform. Composite structural elements have many benefits because of the combination of their properties to behave as a single unit that performs better in both mechanical and thermal behaviour (Lawson 2006). Their many advantages include high stiffness compared to non-composite structural systems, lower bulk density of the structure, good fire resistant behaviour, and economic reasons (Lawson 2006). One of the composite structure elements is the composite slab, which functions to transmit vertical loads and contributes as horizontal bracing to the global structures. Composite slabs require satisfactory fire resistance in line with the building regulations within the region in which they are being constructed.

Composite slabs can be made from steel-concrete, steel-timber or concrete-timber (Designing Buildings 2021). Steel-concrete composite slabs are made by casting either concrete or reinforced concrete on top of a profiled steel deck typically supported by steel beams and steel columns. The steel deck acts as a permanent formwork and a safe working platform (see Figure 1). These elements behave according to the properties of the two materials and their interaction. A composite slab system has many benefits, such as decreasing construction time, saving concrete and reinforcing steel, and good fire resistance (Rackham *et al* 2009). The steel deck also contributes as an additional reinforcement to the slab.

The shape of the steel deck may have an impact on the fire time-resistance (Jiang *et al* 2017). There are many types of steel deck profiles, such as the trapezoidal profile, re-entrant profile and closed profile, as shown in Figure 2. The steel decks are typically galvanised to increase durability by protecting them against corrosion (Hamerlinck 1991).

Steel reinforcement is used in this type of slab either as an anti-crack mesh on the top side of the deck or as an additional reinforcement in the lower part of the slab to raise the shear and the bending moment resistance, as well as an aid to reduce deflections. The steel reinforcement has been shown to increase the fire-resistance time (Bailey 2003).

According to concrete performances, the type of concrete used in steel-concrete composite elements significantly influences the thermal-mechanical behaviour of the

Lakhal A, Bougara A, Benlakehal N. Equivalent fire resistance of composite slab made with lightweight concrete. J. S. Afr. Inst. Civ. Eng. 2025:67(1), Art. #1637, 13 pages. http://dx.doi.org/10.17159/2309-8775/2025/v67n1a2

The *Journal of the South African Institution of Civil Engineering*, which is distributed internationally, is a peer-reviewed, open-access journal licensed under a Creative Commons Attribution Licence (CC BY-NC-ND). Readers may therefore freely use and share the content as long as they credit the original creator and publisher, do not change the material in any way, and do not use it commercially. Copyright of this article remains with the authors.

TECHNICAL PAPER

JOURNAL OF THE SOUTH AFRICAN INSTITUTION OF CIVIL ENGINEERING
ISSN 1021-2019 (print) | ISSN 2309-8775 (online)
Vol 67 No 1, March 2025, Pages 13–25, Paper 1637



ABDENNOUR LAKHAL is a PhD student at the University Hassiba Benbouali in Chlef, Algeria. He is a qualified civil engineer with a solid five years of experience in both site and office work (designing and detailing). His research focuses on numerical simulations of steel and composite buildings under normal and fire conditions, and from these research efforts he was able to submit three conference papers. Along with his research he also tutors steel design and other modules on a part-time basis, as well as co-supervises Master's theses on the optimisation of industrial steel structures.

Contact details:
Structures, Geotechnics and Risks Laboratory
University of Hassiba Benbouali of Chlef
Chlef
Algeria
E: abdennourlakhal@hotmail.com



DR ABDELKADER BOUGARA is a professor in civil engineering at the University Hassiba Benbouali of Chlef in Algeria, specialising in innovative materials and sustainable construction methods. He holds a PhD in Construction Materials and has over 20 years of experience in both academic teaching and research. Dr Bougara's work focuses on developing innovative solutions to enhance the properties of composite structural elements in fire situations. He has published numerous papers in international journals on both concrete technology and composite structures.

Contact details:
Structures, Geotechnics and Risks Laboratory
University of Hassiba Benbouali of Chlef
Chlef
Algeria
E: aekbougara@hotmail.com



DR NOURREDINE BENLAKEHAL is a lecturer in civil engineering at the University Hassiba Benbouali of Chlef in Algeria, with expertise in steel structures, prestressed concrete, and the numerical simulation of structures. Holding a PhD in structural engineering, he has more than 30 years of experience in teaching and research at university level. His research primarily focuses on the numerical simulation of steel and composite structures under fire conditions. Additionally, he investigates optimisation techniques for industrial steel structures in both standard and fire scenarios. He has authored numerous publications on industrial steel buildings and composite structures exposed to fire.

Contact details:
Structures, Geotechnics and Risks Laboratory
University of Hassiba Benbouali of Chlef
Chlef
Algeria
E: n_blk@yahoo.fr

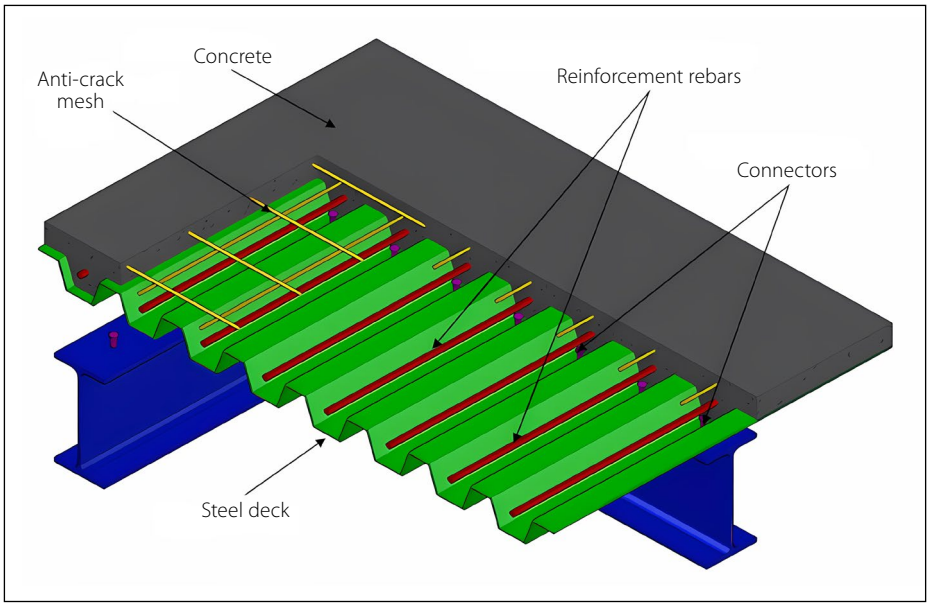


Figure 1 The different elements of a composted slab

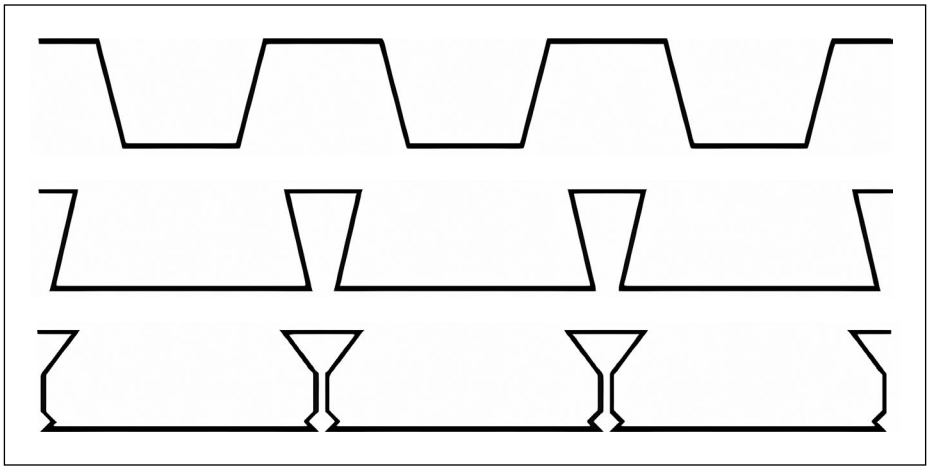


Figure 2 Steel deck profiles

composite element (Fellouh *et al* 2020). In order to increase the fire resistance of the composite element, lightweight concrete (LWC) is well considered due to its low thermal conductivity in fire (Del Coz-Díaz *et al* 2020). Lightweight concrete has low density and thermal conductivity. It is made typically using lightweight aggregate, injecting the concrete mixture with gas bubbles, or substituting fine aggregates. Moreover, lightweight concrete has many advantages, such as that it can be used for insulation as a filling material or as a structural material.

Lightweight concrete must have a compressive strength of at least 17 MPa with a density below 1 840 kg/m^3 (Hedjazi 2020). According to EN1994-1-2:2005, i.e. Eurocode 4 part 1-2 2005 (CEN 2005), the density of unreinforced LWC has to be in the range of 1 600 to 2 000 kg/m^3. Several numerical studies and experimental tests have attempted to evaluate the fire resistance of the composite slabs. Davies and Wang (1994) presented a two-dimensional finite element method to determine the time-dependent temperature distribution. The use of high thermal conductivity to modulate the moisture content around 100°C gives a good prediction of the behaviour as the moisture evaporates. Huang *et al* (2004) conducted a series of analyses on a representative composite floor structure using different patterns of fire protection to the steel beams, including many fire compartments with different sizes and locations. The behaviour was compared to BS5950, and the failure temperatures calculated using a recently published design approach (Bailey's method) (Bailey 2003). They concluded that the slab reinforcements have the ability to sustain the tensile stress, and that the current structural fire design code, based on standard fire tests on isolated structural members, cannot properly represent the structural behaviour of real buildings in fire conditions.

Shah and Vadik (2014) reported a parametric study of seven composite decks with and without embossment. Employing a three-dimensional model using ANSYS (ANSYS n.d.) they discovered that the deflection and the stress in the slab without embossment are higher than in the slab with embossment. The thickness of the profiled sheet has a considerable effect on the deflection and stress of the composite slab. Jiang *et al* (2017) presented a numerical study for heat transfer in composite floor slabs with trapezoidal profiled steel considering the thermal boundary conditions, thermal properties of the materials and the slab geometry. They showed that the temperature distribution is highly non-uniform due to the presence of the ribs. Li *et al* (2017) performed experimental work on four composite slabs supported by one unprotected secondary beam with different ribs orientation and locations of the reinforcement rebars. From this investigation they concluded that the highest reinforcement and steel deck temperatures occurred during the cooling phase. The location of the reinforcement had a significant influence on its temperature. For the fire insulation criterion, the temperature on the unexposed side of all the tested slabs was less than 100°C for a heating duration of up to 100 min, compared to a calculated fire resistance of 93 min based on the Eurocode 4 method (CEN 2005). Piloto *et al* (2018) evaluated the fire resistance of trapezoidal rib slabs using two geometries with eight slab thicknesses of normal-weight concrete (NWC) by using the numerical simulation and simple method presented in Eurocode 4 part 1-2 Annexe D (CEN 2005). They found that the simulation method gives a lower fire resistance compared to the Annex D method in most cases. From their results, they proposed a new, safer formula to define fire resistance.

Jiang *et al* (2019) carried out a numerical study on the composite slabs made with NWC and LWC, taking into account the effect of the moisture content (in the range of 3% to 10%). Considering the effect of moisture content and slab geometries, they concluded that the method given in the Eurocode 4 (CEN 2005) was under-conservative for up to 35% and over-conservative for up to 46% in predictions of the fire resistance of composite slabs. Del Coz-Díaz *et al* (2020) carried out an experimental study on composite slabs made with NWC and LWC using a manufactured furnace. They deduced that the heat-transfer phenomenon is influenced by the moisture content and permeability of concrete. Also, the temperature does not increase until all the water has been removed by evaporation. Moreover, the steel decking profile acts as a barrier preventing explosive spalling.

Table 1 Literature review summary

Authors	Nature of the work	
	Experimental work results	Numerical work results
Davies & Wang (1994)	/	A good prediction of the fire behaviour is achieved with high thermal conductivity.
Huang *et al* (2004)	/	Structural fire design codes cannot properly represent the structural behaviour of real buildings in fire conditions.
Shah & Vadik (2014)	/	The deflection and the stress in the slab without embossment are higher than the slab with embossment.
Li *et al* (2017)	Highest temperatures of reinforcement and steel deck occurred during the cooling phase.	/
Jiang *et al* (2017)	/	The temperature distribution on the composite slab is highly non-uniform.
Piloto *et al* (2018)	/	The simulation method gives a lower fire resistance compared to the Annex D method in most cases.
Jiang *et al* (2019)	/	EC4 (CEN 2005) was under-conservative up to 35% and over-conservative up to 46% predictions of fire resistance of composite slabs.
Del Coz-Díaz *et al* (2020)	The heat transfer phenomenon is influenced by moisture content and permeability of concrete.	/
Piloto *et al* (2021)	/	The numerical results are close to those of the experimental results when considering the airgap effect.
Balsa *et al* (2022)	/	LWC moisture and the mechanical effect of the airgap are recommended to be included for future studies.
Zhao *et al* (2022)	The RAC releases more vapour than NWC.	The thermal convection at the rib location and the thermal resistance at the steel-concrete interface in the model were recommended to be 1 W/m^2·K and 0.01 (m^{2}K)/W, respectively.

However, they noticed that debonding of the profile steel takes place. A three-dimensional simulation based on full-scale and multi-domain slabs applying both ANSYS and MATLAB software programs was performed by Piloto *et al* (2021). They evaluated the thermal effect on the composite slabs with trapezoidal steel decks using NWC, taking into account the effect of the debonding between the concrete and the steel deck. This debonding was simulated by an airgap. As a result, they concluded that, when considering the airgap effect, the numerical results are close to those of the experimental results. Thus, a new formula has been proposed for the calculation of the fire resistance. Recently Balsa *et al* (2022) developed more realistic computational models to represent the thermal behaviour of composite slabs under fire conditions using MATLAB. The main objective of this study was to determine the temperature distribution on the slab elements and to compare them with the Eurocode 4 (CEN 2005). Forty numerical simulations were performed to analyse the composite slabs made with NWC and LWC, considering the effect of the airgap. This work resulted in a new calculation proposal for determining the temperature in the steel deck components. They recommended including the LWC moisture and the mechanical effect of the airgap for future studies. Recently, Zhao *et al* (2022) performed four full-scale fire tests for a duration of 90 min on composite slabs including closed profiles steel decking and recycled aggregate concrete (RAC). A numerical investigation using ABAQUS software was used in this study, taking into account the airgap and the effect of the moisture content. It was concluded that the RAC releases more vapour than NWC. Therefore, by using coarse recycled aggregate, a lower temperature within the concrete results, depending on the thermal properties, the airgap and the moisture content.

Table 1 provides a summary of the conclusions drawn from the above literature.

OBJECTIVE

Based on the aforementioned studies, the main objective of this study was to analyse the fire resistance time of lightweight concrete (LWC) using the numerical simulation and simple method presented in Eurocode 4 part 1-2 Appendix D (CEN 2005). This study includes different parameters, such as the thickness of the concrete, re-entrant and trapezoidal steel decks, airgap, and the moisture content. The current work is based on two calculation methods, which are the simple method given in Appendix D of Eurocode 4 part 1-2 (CEN 2005) and the numerical method based on the 3D finite elements model using ANSYS (ANSYS n.d.).

METHODOLOGY

The simple method of Eurocode 4

Eurocode part 1-2 annex D, i.e. Eurocode 4 part 1-2 2005 (CEN 2005) mandates the verification of the insulation criterion "I," which ensures that fire does not spread to the unexposed surface of the element. Temperature rise must not exceed an average of 140°C (T_{int} + 140°C) on the unexposed surface above the initial temperature, or a maximum of 180°C (T_{int} + 180°C) above the initial temperature at any point of the unexposed surface. The verification is done upon time using Equations 1 to 3:

$$t_i = a_0 + a_1 h_1 + a_2 \phi_{up} + a_3 \frac{A}{L_r} + a_4 \frac{1}{l_3} + a_5 \frac{A}{L_r} \frac{1}{l_3} \quad (1)$$

$$\frac{A}{L_r} = \frac{h_2 \left(\frac{l_1 + l_2}{2} \right)}{l_2 + 2\sqrt{h_2^2 + \left(\frac{l_1 - l_2}{2} \right)^2}} \quad (2)$$

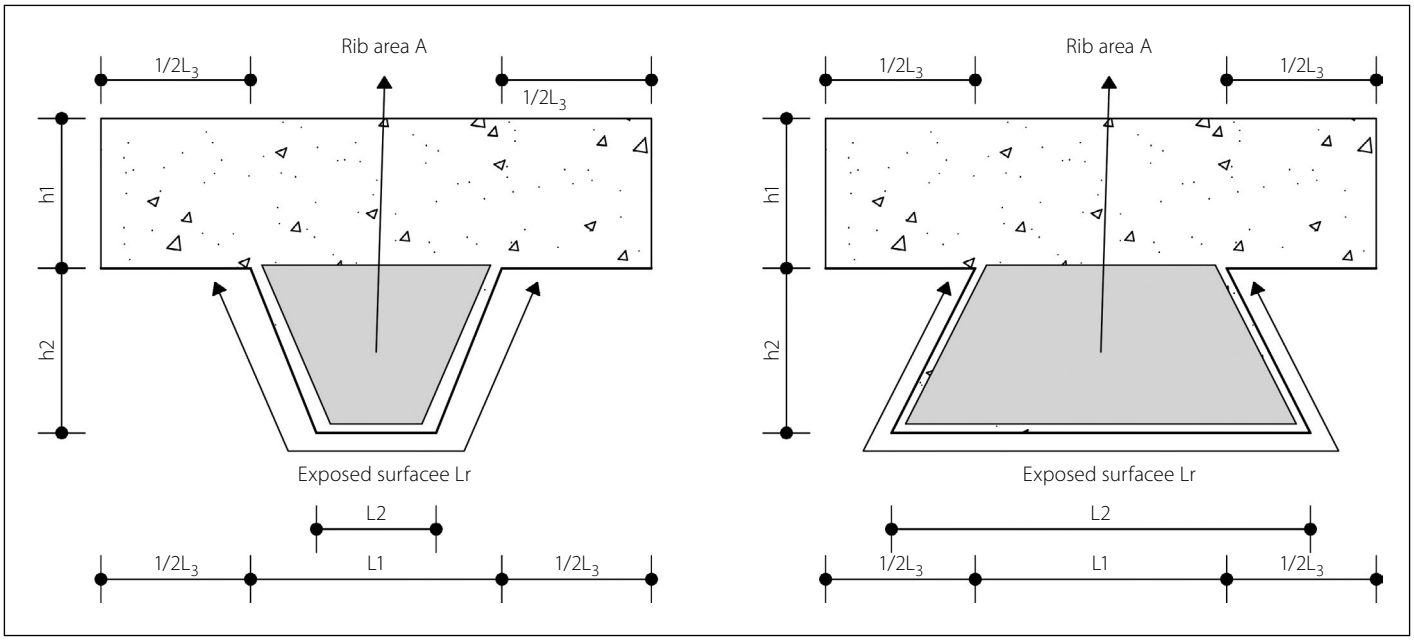


Figure 3 Definition of the rib geometry factor

$$\phi_{up} = \frac{\left[\sqrt{h_2^2 + \left(l_3 + \frac{l_1 - l_2}{2}\right)^2} - \sqrt{h_2^2 + \left(\frac{l_1 - l_2}{2}\right)^2}\right]}{l_3} \quad (3)$$

Where: h_1 represents the thickness of the continuous upper portion of the slab, ϕ_{up} is the view factor of the upper flange of the steel decking, and $\frac{A}{L_r}$ demonstrates the rib geometry factor. Lastly, the coefficients a_0 to a_5 are specified in Eurocode 4 for both NWC and LWC (see Figure 3).

Table 2 regroups the coefficient a_i for both NWC and LWC. These coefficients, related to the type of concrete, are used to determine the fire resistance of the composite slabs according to the thermal insulation criterion.

Table 2 Coefficients for the determination of fire resistance according to thermal insulation criterion

Concrete type	a_0 (min)	a_1 (min/mm)	a_2 (min)	a_3 (min/mm)	a_4 (min.mm)	a_5 (min)
NWC	–28.8	1.55	–12.6	0.33	–735	48.0
LWC	–79.2	2.18	–2.44	0.56	–542	52.3

Numerical simulation method

The finite element method requires the solution of the heat diffusion Equation 4:

$$\frac{\partial^2 T}{\partial x^2} + \frac{\partial^2 T}{\partial y^2} + \frac{\partial^2 T}{\partial z^2} + \frac{\dot{q}}{\lambda} = \frac{\rho c}{\lambda}\frac{\delta T}{\delta t} \quad (4)$$

The equation can be simplified for homogeneous isotropic materials and unidirectional heat transfer, resulting in the following form:

$$\lambda \frac{\partial^2 T}{\partial y^2} = \rho c \frac{\delta T}{\delta t} \quad (5)$$

Where λ is the thermal conductivity, T is the temperature of the element, c is the specific heat of the material, and ρ is the material's density.

To solve Equations 4 and 5, the heat transfer boundary conditions should be given in Equation 6:

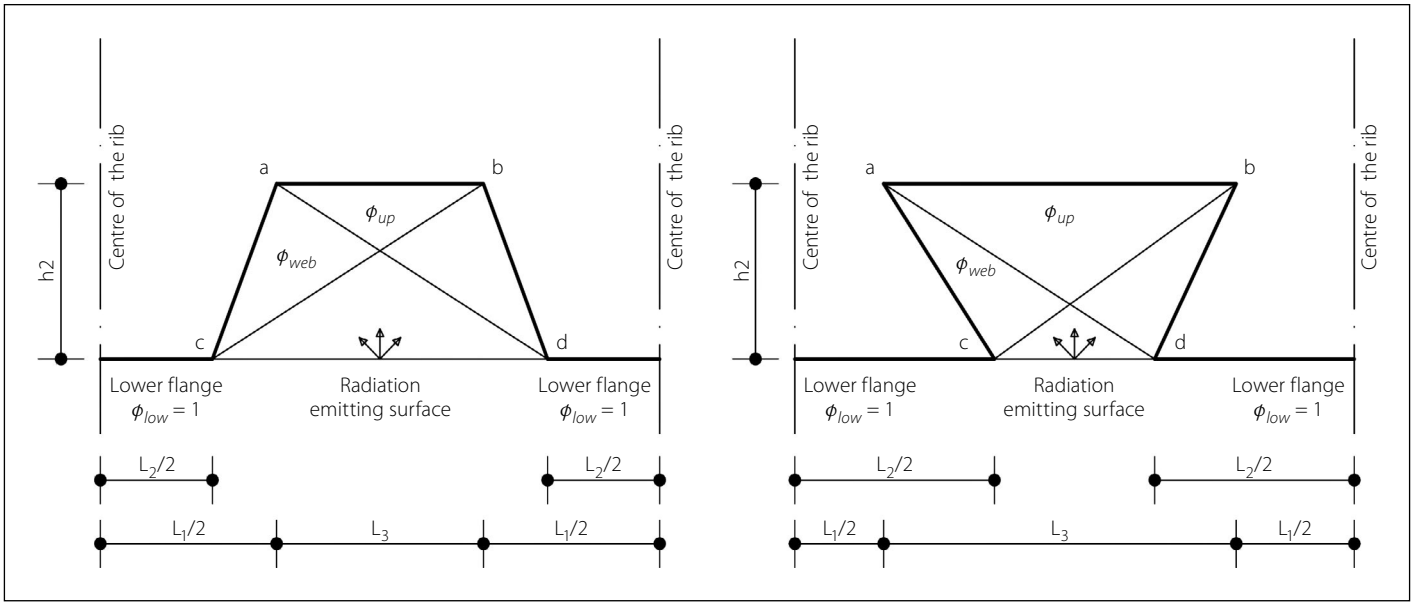


Figure 4 Schematic for the calculation of view factor (Jiang *et al* 2017)

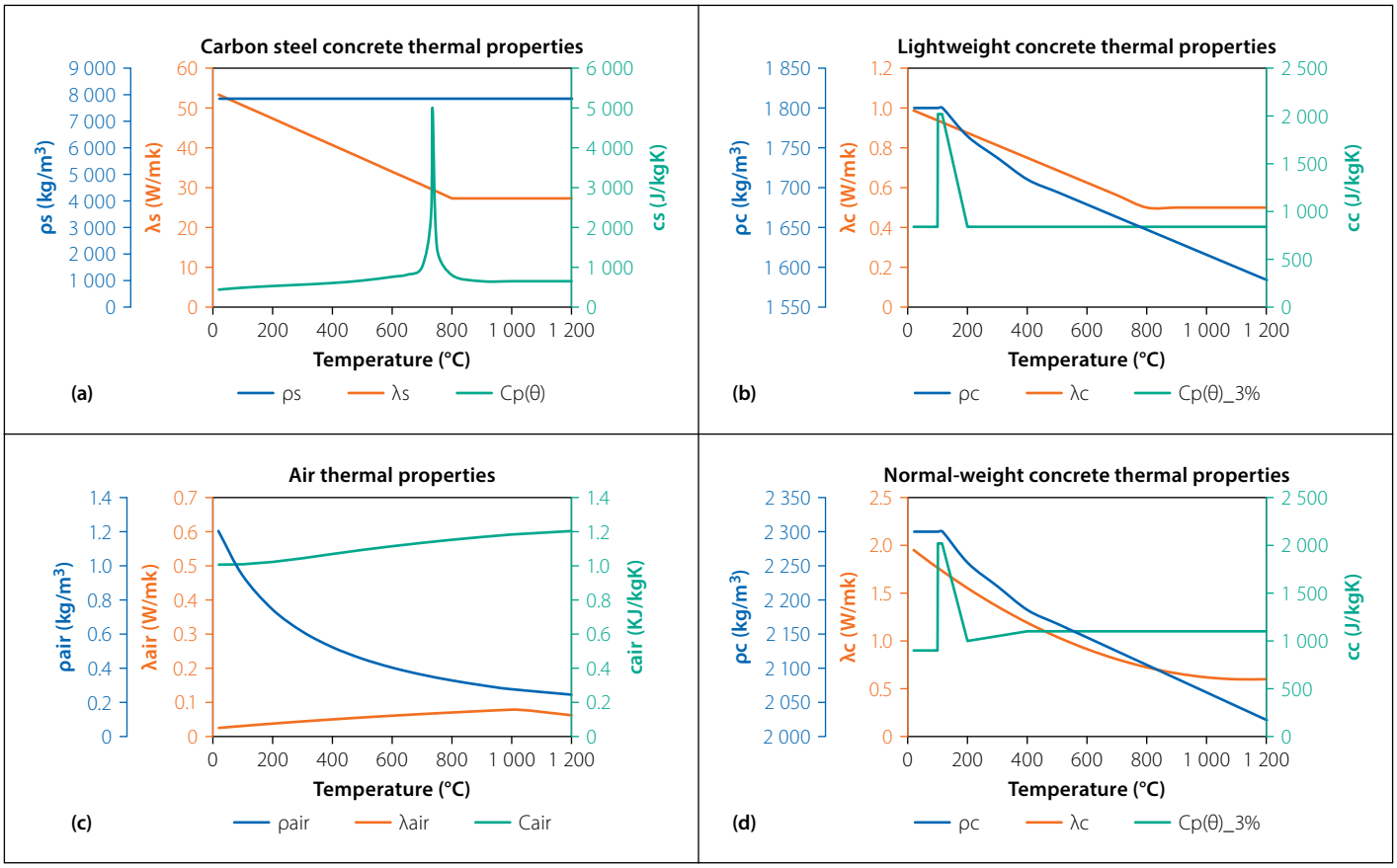


Figure 5 Thermal properties of (a) carbon steel, (b) LWC, (c) air, (d) NWC

$$\dot{h}_{net,d} = \dot{h}_{net,r} + \dot{h}_{net,c} = \sigma\phi\varepsilon_m\varepsilon_f[(T_g + 273)^4 - (T_m + 273)^4] + \alpha_c(T_g - T) \quad (6)$$

In Equation 6 $\dot{h}_{net,r}$ and $\dot{h}_{net,c}$ represent the heat flux from radiation and convection respectively, σ is Stefan-Boltzmann's constant, ε_f is the fire emissivity equal to 1, ε_m is the emissivity of the materials which is equal to 0.7, θ_g symbolises the gas temperature, θ_m represents the materials temperature, and α_c defines the convection coefficient. Finally, the view factor ϕ is purely a geometrical parameter. It represents the portion of the radiative heat flux, which leaves the surface and strikes another surface (ANSYS n.d.). For the lower flange this is equal to 1, as well as for the upper flange which is calculated referring to Equation 3 and for the web which is calculated according to Equation 7. Also see Figure 4.

$$\phi_{web} = \frac{ad + cb - ad - cd}{2ab}$$

$$= \frac{\left[\sqrt{h_2^2 + \left(\frac{l_1 - l_2}{2}\right)^2} + (l_3 + l_1 - l_2) - \sqrt{h_2^2 + \left(l_3\frac{l_1 - l_2}{2}\right)^2}\right]}{2\sqrt{h_2^2 + \left(\frac{l_1 - l_2}{2}\right)^2}} \quad (7)$$

CHARACTERISTICS OF THE MATERIALS

Each component of the composite slab is modelled considering various materials, including carbon steel for the steel deck, air for the airgap, and concrete made with both lightweight concrete (LWC) and normal-weight concrete (NWC). The results of the different effective characteristics are shown in Figure 5.

These figures reveal that most of the effective characteristics are dependent on the temperature evolution according to the assumption that the authors have made in the current study. It should be noted that the specific heat for the LWC is represented by a linear constant curve when the moisture is equal to 0. However, when the moisture content is considered, a peak of 2 020 J/kg K appears at temperatures ranging from 100°C to 115°C for both concretes; and then the specific heat decreases linearly up to 200°C.

According to Figure 6, the specific heat of lightweight concrete shows no

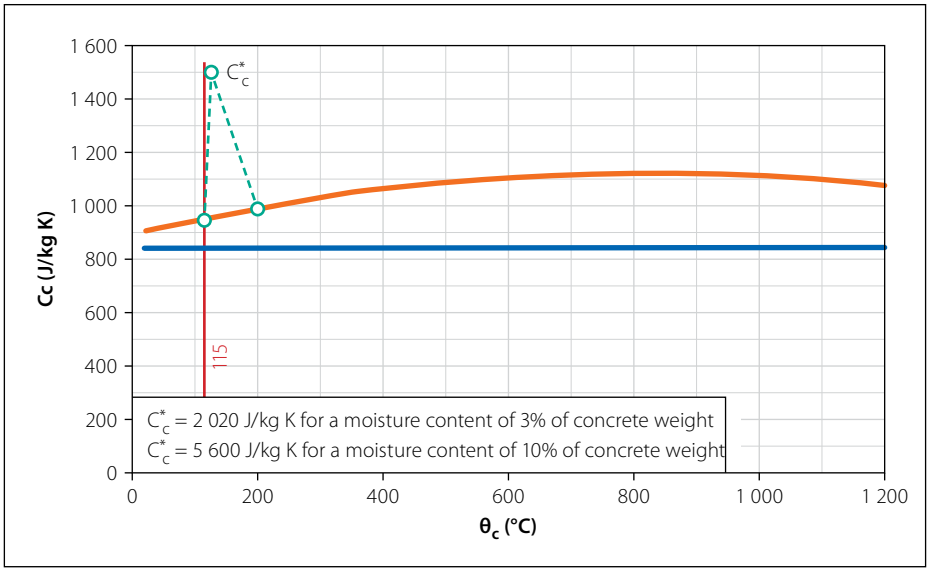


Figure 6 Specific heat of normal-weight concrete (NWC) and lightweight concrete (LWC) as a function of the temperature as in Eurocode 4 (CEN 2005)

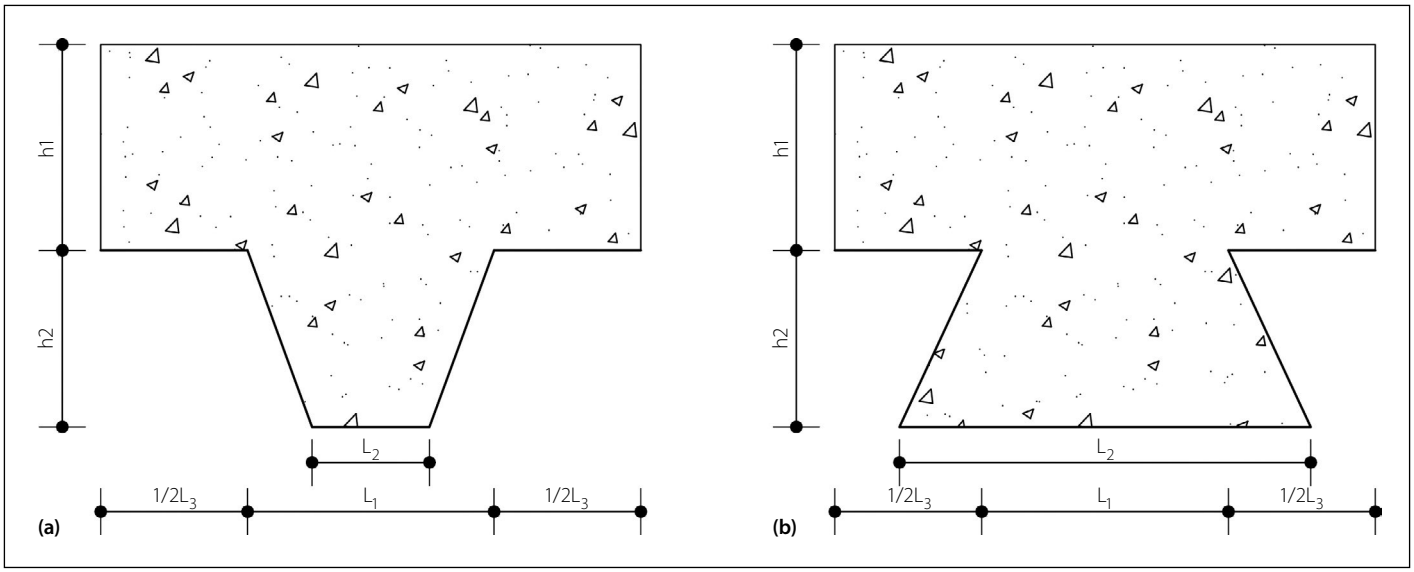


Figure 7 Composite slab geometry (a) trapezoidal profile (b) re-entrant profile

peak, indicating the absence of moisture content. In this study, the authors varied the moisture content percentage to compare it with normal-weight concrete (NWC).

MODELLING

The simulations were conducted using mechanical APDL (ANSYS Parametric Design Language) (Piloto *et al* 2018; 2021), which is powerful software applied in engineering to solve both linear and nonlinear problems, such as the thermal conditions in either the transient regime and steady-state regime. It is used for two-dimensional or three-dimensional geometries. This analysis is performed taking into consideration boundary conditions, steel deck geometries and mesh convergence.

Numerical model boundary conditions

The lower edge of the slab is assumed to be submitted to standard fire conditions for a considerable time to satisfy the insulation criterion, where the time step is 60 s and may be reduced to 1 s. An initial temperature of 20°C is applied on all nodes. The heat transfer by convection on the exposed side is represented by the coefficient α_c = 25 W/m²K (CEN 2002; Balsa *et al* 2022; Piloto *et al* 2018). Regarding the unexposed side (the upper edge of the slab), a coefficient of heat transfer by convection equal to α_c = 9 W/m² is taken to include the radiation effect as well (CEN 2002; Balsa *et al* 2022; Piloto *et al* 2018).

The geometry of the composite slab is defined by five parameters (h_1, h_2, L_1, L_2, L_3), as shown in Figure 7. These respectively represent the height of the concrete above the steel deck, the depth of the steel deck, the length of the lower flange, the width of the rib measured from the top (between two upper flanges), and the length of the upper flange.

For the parametric study, four distinct deck geometries were employed. Two of them were re-entrant Multideck 50 and Cofrastar 40, and the other two trapezoidal geometries were Polydeck 59S and Hi-Bond 55. These steel decks are represented in Figure 8.

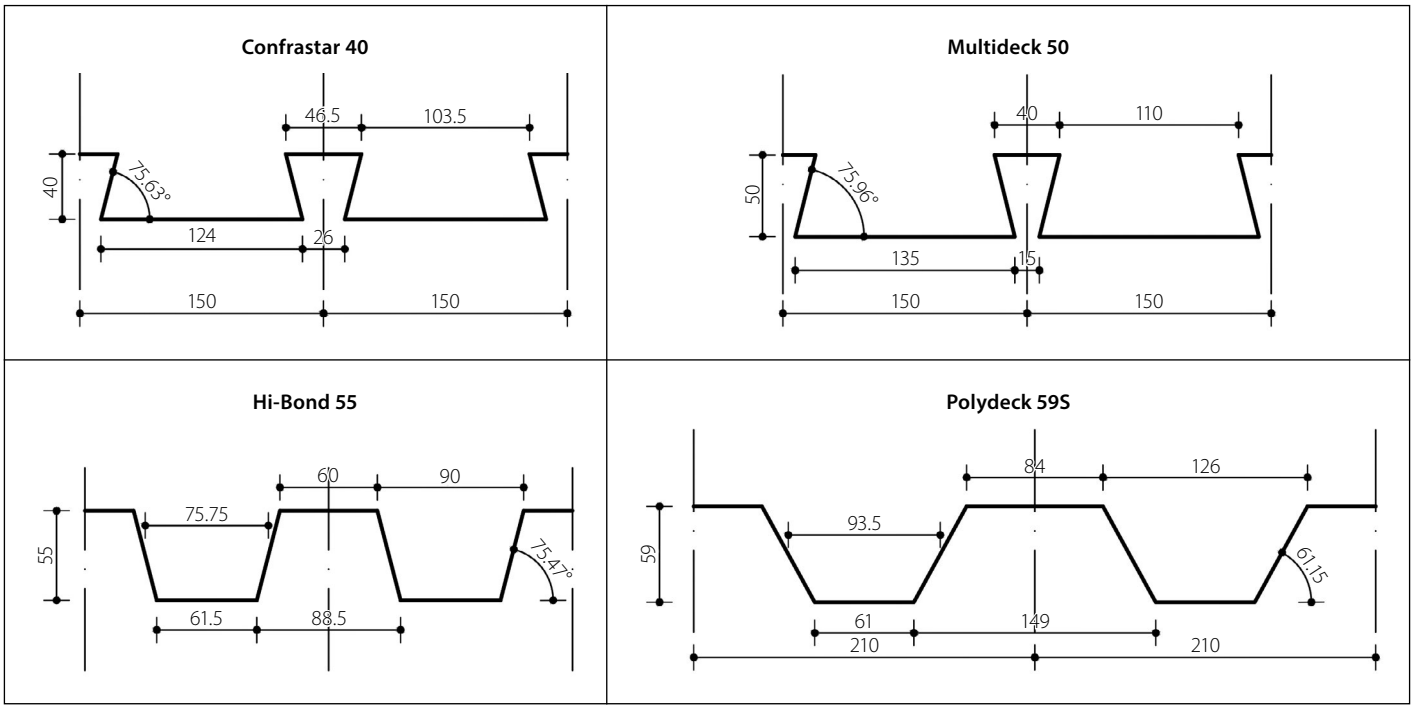


Figure 8 Still decks geometric characteristics and dimensions (mm)

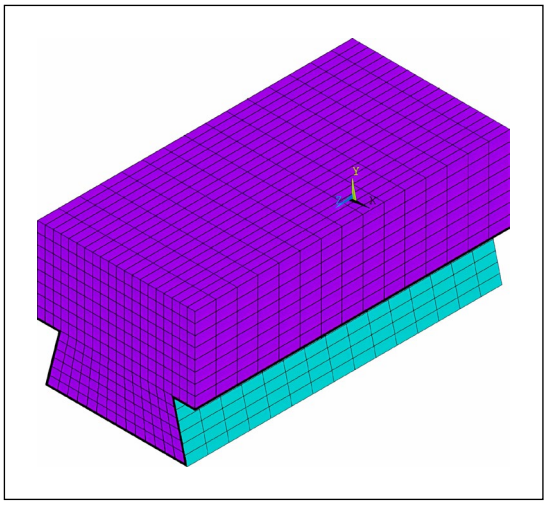


Figure 9 Finite element meshes

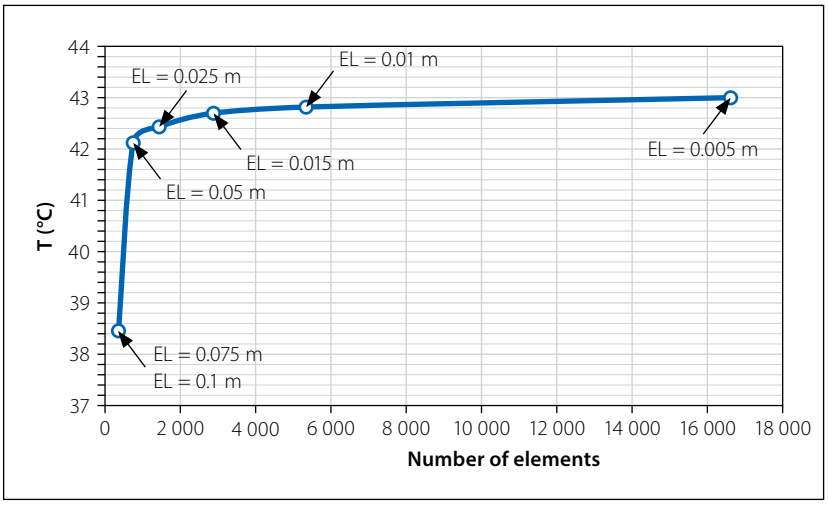


Figure 10 Mesh convergence study

The mesh convergence study

The model was created using a finite element known as SOLID70 to simulate each component, namely the steel deck, the concrete, and the airgap. SOLID70 is a three-dimensional finite element with 8 nodes, each having a single degree of freedom, which is temperature (see Figure 9).

The mesh convergence study was performed using several element lengths to determine when the model converges to a constant value. The results represented in Figure 10 are for a transient regime, and the fill material is NWC using a time step of 60 s which can be reduced to 1 s.

From the results above, it is evident that the use of greater element lengths leads to inaccurate results (EL > 0.05 m). The results became more appreciable when decreasing the element lengths; smaller element lengths lead to a dense number of elements. Thus, the solution requires more time, computational effort, and considerable memory consumption. To make the mesh convergence study more efficient, the authors assumed that EL = 0.01 m satisfies both the criteria of computational effort and convergence value. It is to be noted that the number of elements used in this study reaches around 5 500 elements, which demonstrates the accuracy of the model, as shown in Figure 10.

PARAMETRIC STUDY CHART

To clearly explain the work, a chart diagram was created for the parametric study that was conducted (see Figure 11). It starts with the selection of the LWC material presented in Eurocode 4 part 1-2 (CEN 2005), applied on both trapezoidal and re-entrant steel deck, and then for the geometry, which gives the best value of time resistance. Regarding the geometrical section the authors have varied the airgap thickness, the moisture content percentage, the thermal conductivity and the density.

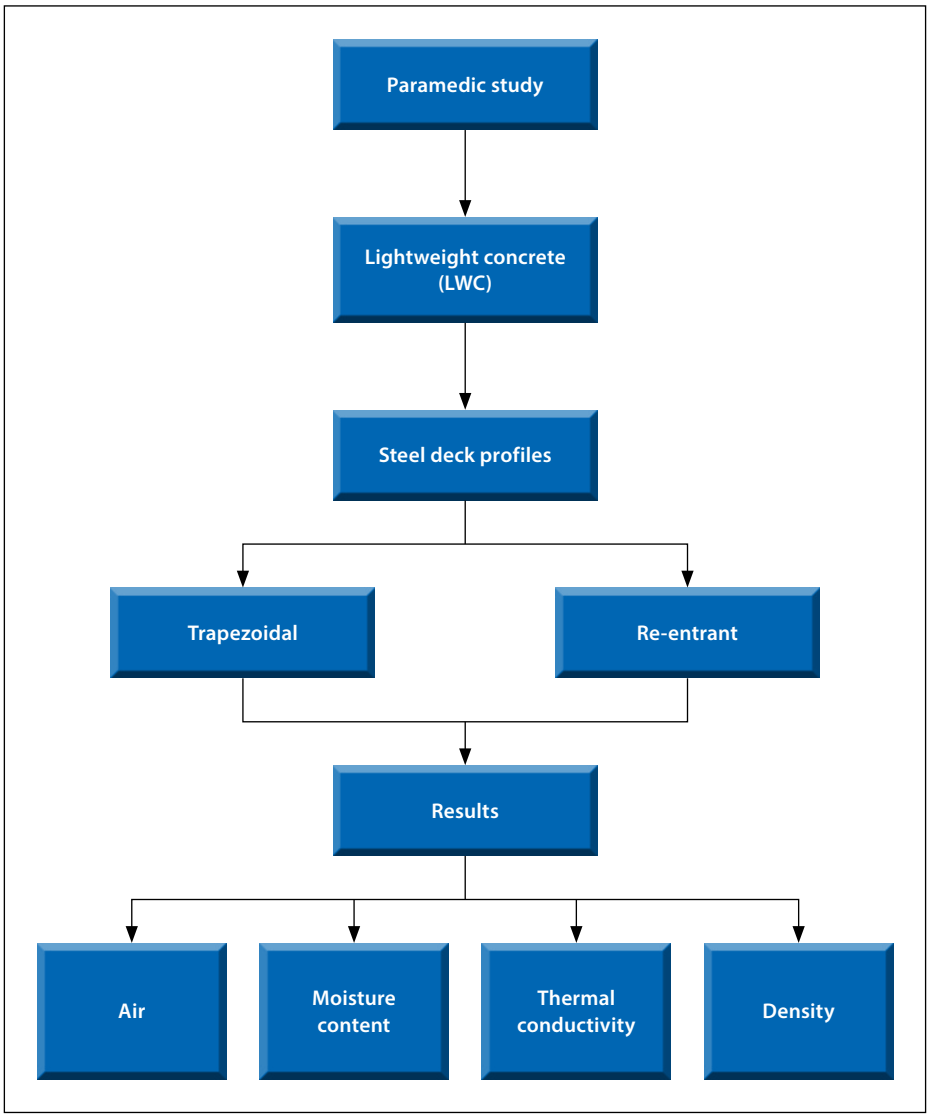


Figure 11 Parametric study chart

NUMERICAL RESULTS

The parametric study of the thermal analysis of the slab made with lightweight concrete (LWC) examined the effects of several factors, namely the geometry of the steel deck, the airgap between the steel deck and concrete, the moisture content, and the density and thermal conductivity of the concrete.

The maximum temperature is the highest value of the temperature measured

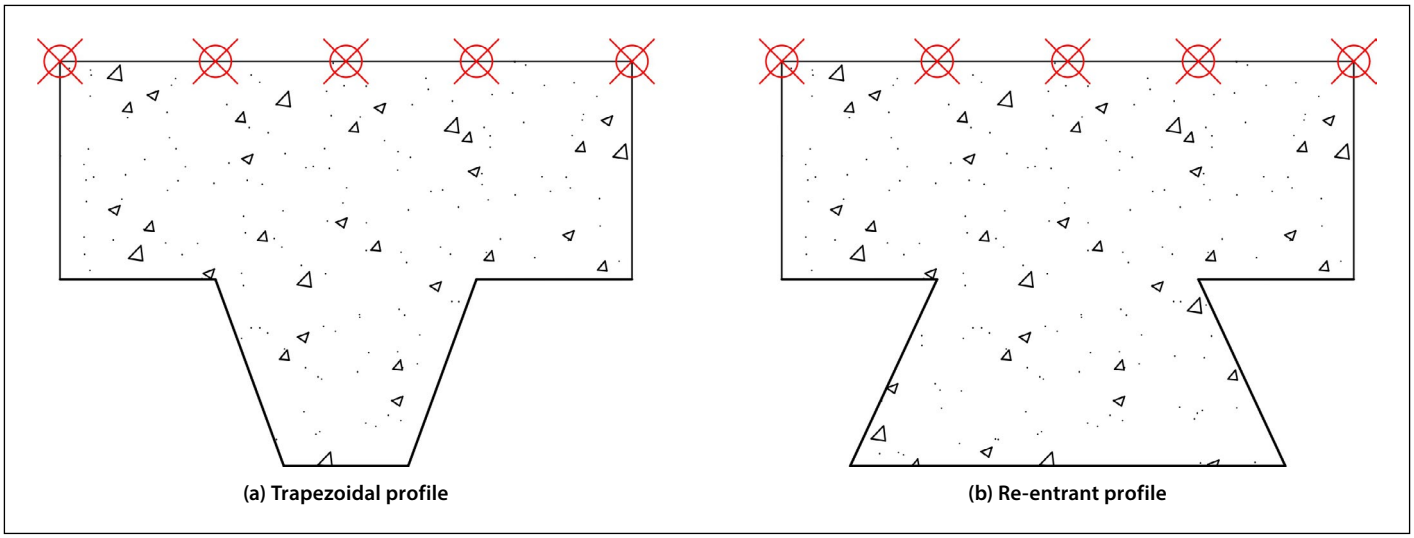


Figure 12 Measuring points

on the unexposed side of the slab, whereas the average temperature is the mean of the given temperatures measured on the unexposed side of the slab on the points presented in Figure 12.

Figure 13(a) represents the evolution of the average and the maximum temperatures of the re-entrant composite slab (Cofrastar 40) for the different slab thicknesses. Figure 13(b) shows the temperature distribution inside the slab, with h_1 the depth of the concrete on top of the steel deck equal to 80 mm. One can see that the temperature increases with the decrease of the concrete thickness because of the reduction of the thermal mass. The maximum temperature and the average temperature for all slab thicknesses considered in this study exceed the temperature limited by the insulation criterion as per Eurocode 4 part 1-2 2005 (CEN 2005). It is to be noted that the moisture content and the airgap are neglected in this case (the airgap thickness δa is equal to 0).

Figure 14(b) illustrates the temperature distribution inside the slab made with LWC, with the depth of the concrete on the top of the steel deck h_1 = 80 mm taking the same conditions as in the section described above. Also, Figure 14(a) shows the same tendency as in Figure 13(a). It is observed that the maximum temperature and the average temperature for all slab thicknesses exceed the temperature limited by the insulation criterion on the considered points, i.e. Eurocode 4 Part 1-2 2005 (CEN 2005). Since the results of the temperature distribution are approximately similar in both composite sections with different steel decks, it seems that this temperature distribution is independent of the geometrical form of the slab regarding the considered points (see Figure 12).

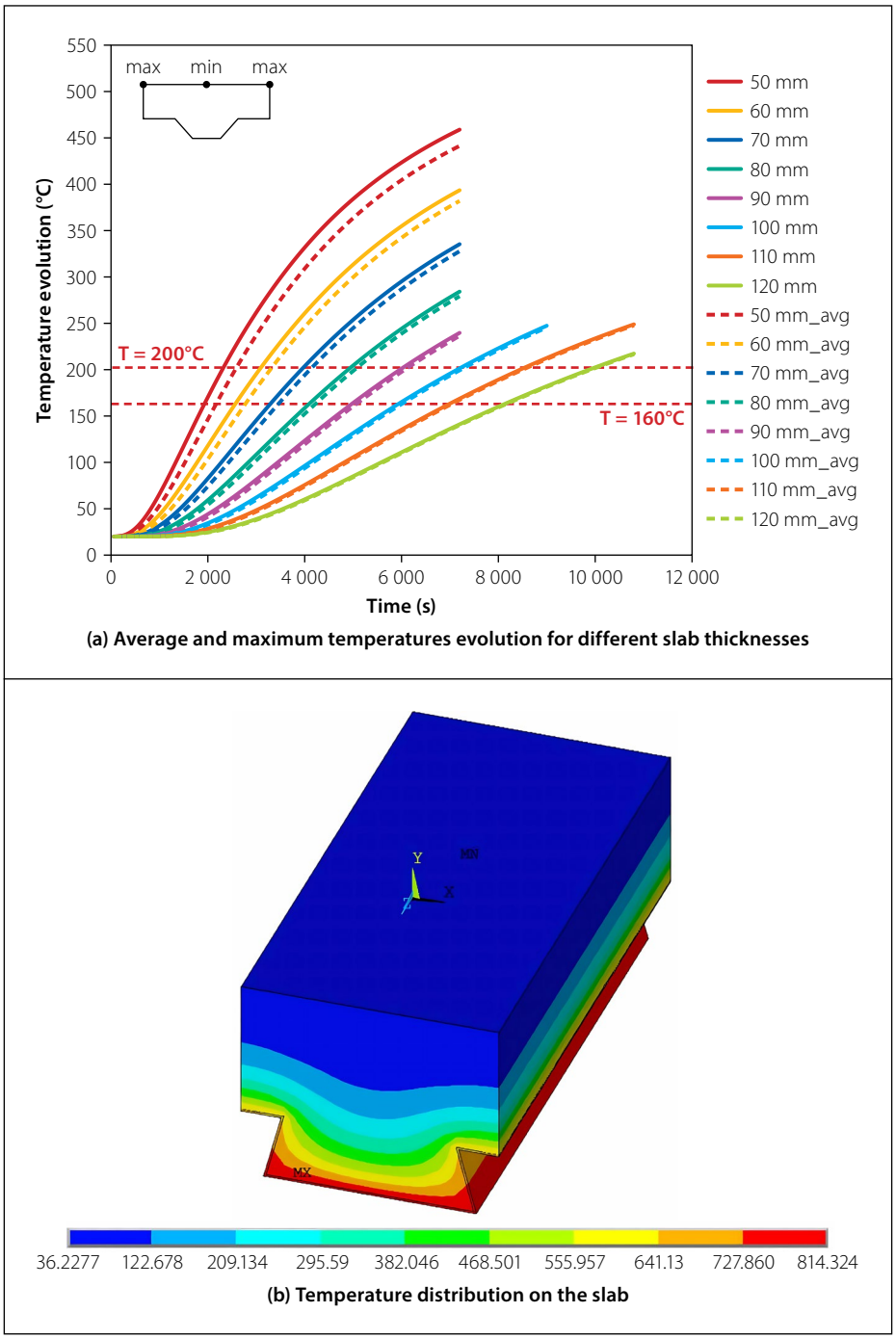
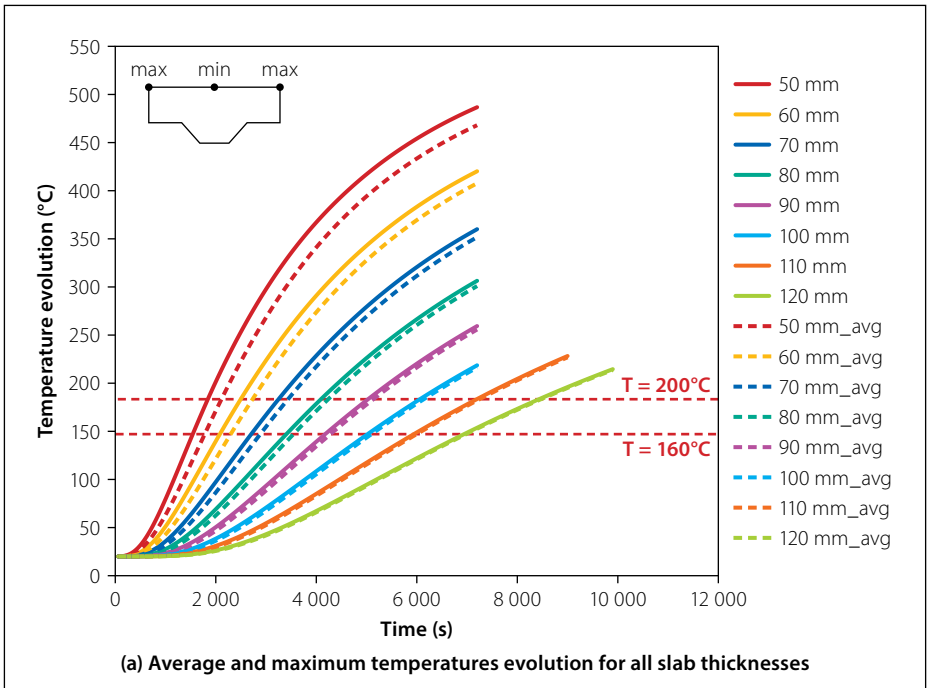
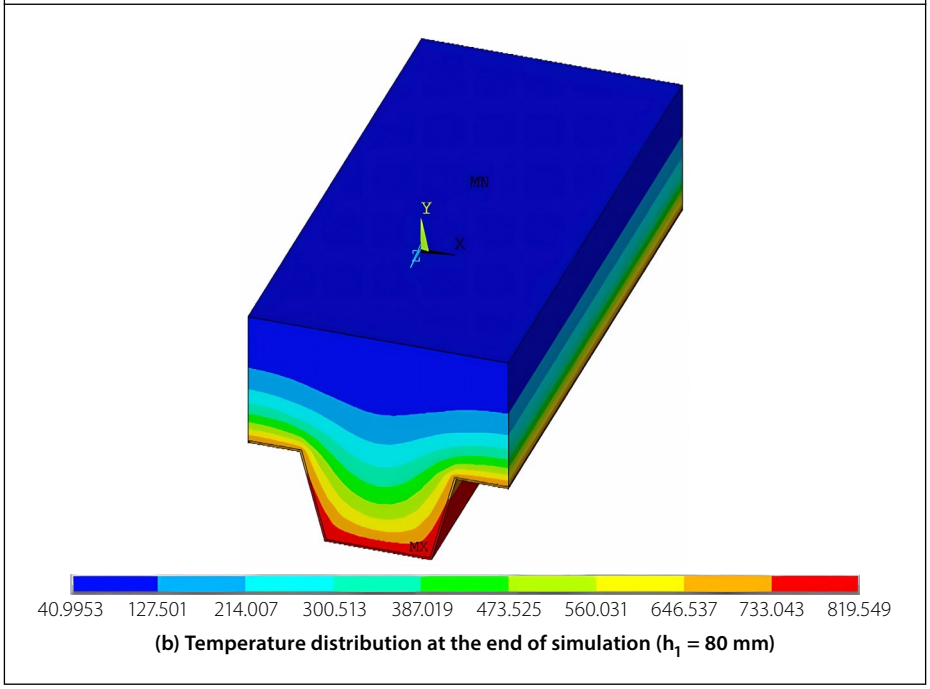


Figure 13 Results of the Cofrastar40 made with LWC, M.C = 0% and δa = 0 mm



(a) Average and maximum temperatures evolution for all slab thicknesses



(b) Temperature distribution at the end of simulation (h_1 = 80 mm)

Figure 14 Results of the Hi-Bond 55 made with LWC, M.C = 0% and δa = 0 mm

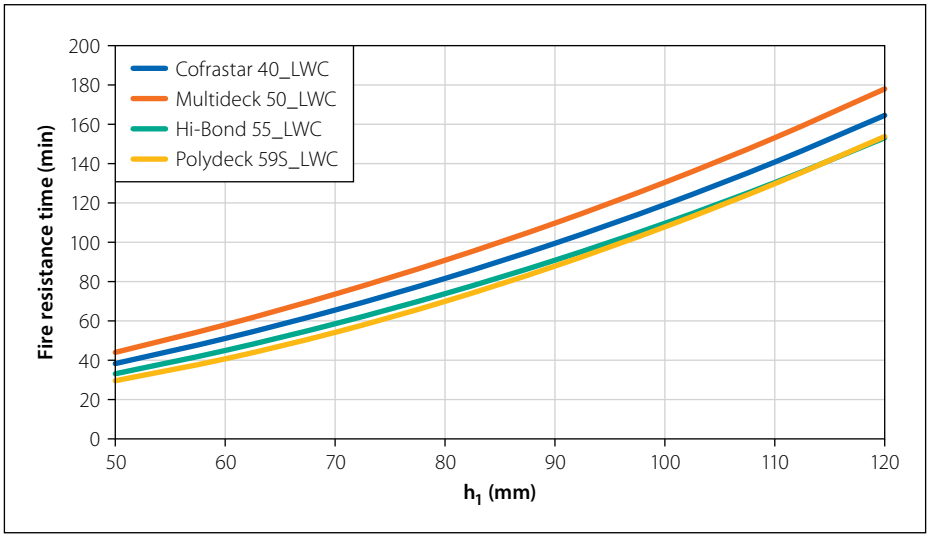


Figure 15 Resistance time comparison between trapezoidal and re-entrant steel decks made with LWC

Effect of the steel deck geometry

The geometry of the steel deck is considered when evaluating the fire resistance time of the composite slabs. A set of 32 numerical simulations were carried out varying the value of the topping concrete (h_1) from 50 mm to 120 mm for both trapezoidal and re-entrant composite slabs (two different sections for each profile). The effects of the airgap, moisture content, thermal conductivity and density of concrete are not considered in this case.

Figure 15 shows the resistance time evolution for all composite slabs with different steel decks made with LWC as a function of the topping concrete thickness. According to this figure, the time resistance of the re-entrant steel deck is better than the trapezoidal steel deck.

Effect of the airgap

In order to show the influence of the airgap on the fire resistance time, the characteristics of the LWC of the composite slab, namely the moisture content, the density and the thermal conductivity, are kept constant and the airgap between the steel deck profile and the LWC varies from 0 mm to 1 mm. In the literature, 0.5 mm is commonly used for the airgap (Balsa *et al* 2022).

The evolution of the fire resistance time of the composite slab as a function of the thickness of the slab for the airgap values is plotted in Figure 16. It is observed that the fire resistance time of the composite slab increases with the increase of the airgap. At a given airgap, the fire resistance time increases with the increase of the slab thickness.

The fire resistance time results obtained using the Eurocode 4 method (CEN 2005) are greater than those obtained using the simulation method in this study. This difference may be attributed to the initial boundary conditions taken at the beginning of the calculation (Jiang *et al* 2017).

To clarify the effect of the airgap on the fire resistance time of the composite slab, Figure 17 was plotted. An increase of approximately 10 min of the fire resistance time is reached when the airgap is taken equal to 1 mm for 50 mm of slab thickness. However, for the thickness of 100 mm, an airgap of 0.5 mm and 1 mm is needed to produce an increase of the fire resistance time of 8 min and 15 min, respectively. It is evident that the increase of the void between the steel deck profile and the topping concrete leads to the increased fire resistance time of the composite slab.

Effect of the moisture content

In this section, all parameters are kept constant except for the moisture content, which varies from 0% to 6%. It is noted that beyond 6% of the moisture content, the numerical simulation of the thermal analysis does not converge. Some authors believe that lack of convergence is linked to the way moisture content is modelled (Wickström 2016).

The influence of the variation of the moisture content (MC) of the LWC on the evolution of the fire resistance time is illustrated in Figure 18. For a given slab thickness, a proportional increase in fire resistance is observed with increased moisture content. This improvement of the fire resistance is associated with the peak that appeared in the specific heat curve (see Figure 5). It is reported in the literature (Del Coz-Díaz 2020) that the free water inside the LWC evaporates during the heating. This phenomenon leads to a delay of the heating process. It can be seen that the results of the Eurocode 4 (CEN 2005) method are comparable to the results of the numerical simulation starting from 75 mm when taking 3% of MC and 0.5 mm airgap.

According to the results found, with 6% of MC, the fire resistance time can reach the value of four hours.

Effect of the thermal conductivity

This section examines the effect of the variation of the thermal conductivity. However, the other influencing parameters are kept constant. Table 3 regroups the values of the thermal properties.

Figure 19 illustrates the impact of the variation of the initial thermal conductivity of the LWC on the fire resistance time as a function of the topping concrete thickness. It can be seen that the lower density of the concrete (lower thermal conductivity) leads to higher fire resistance time. A decrease of the density of the concrete slab from 1 922 kg/m^3 to 1 822 kg/m^3 gives an enhancement of the fire resistance time up to 12% for a 100 mm thickness slab. The increase in the fire resistance time can

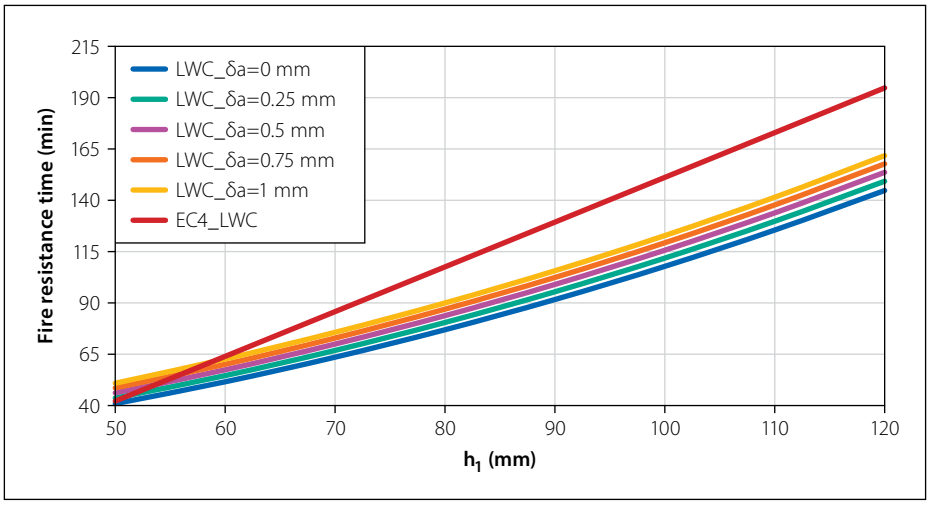


Figure 16 Fire resistance time of the composite slab versus the thickness of the slab with different airgap values

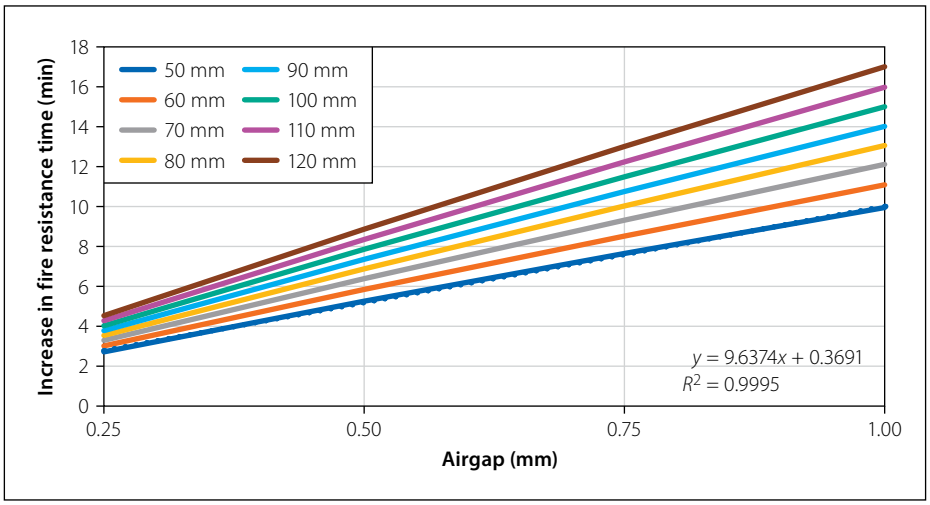


Figure 17 The increase in fire resistance time on the function of the airgap

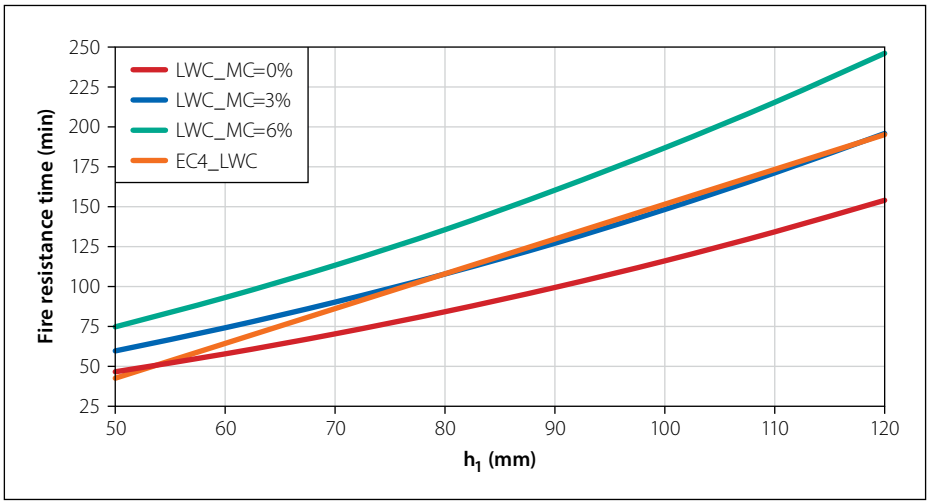


Figure 18 Resistance time comparison between three LWCs made with different moisture content

Table 3 Parameters for the thermal conductivity effect study

Parameter	LWC-1	LWC-2	LWC-3
Moisture content	LWC: 3%	LWC: 3%	LWC: 3%
Density (function of temp)	*LWC: 1 920 kg/m^3	**LWC: 1 822 kg/m^3	*LWC: 1 600 kg/m^3
Thermal conductivity (function of temp)	*0.9 to 1.3 W/m.K (1.1 was taken)	**0.92 W/m.K	*0.68 to 0.89 W/m.K (0.79 was taken)
Airgap	0.5 mm	0.5 mm	0.5 mm
* Cavalline *et al* 2017 ** Punlert *et al* 2017			

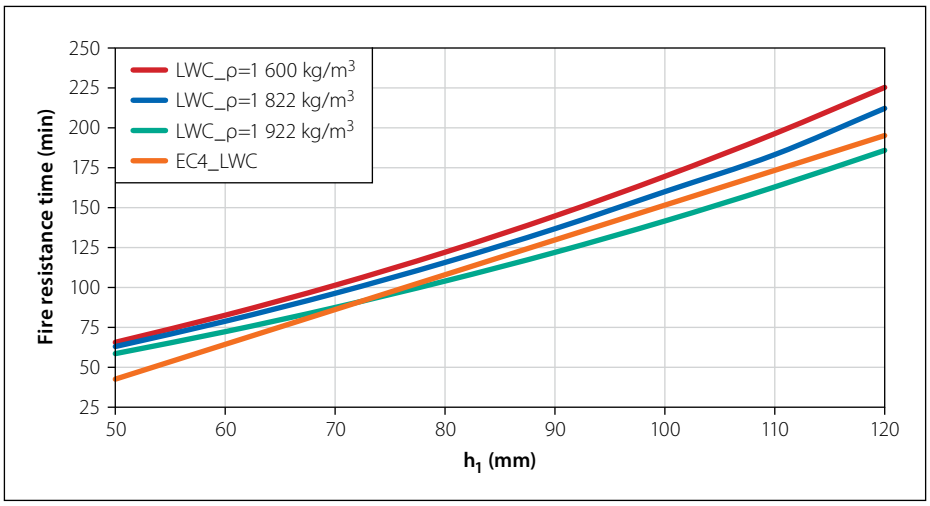


Figure 19 Resistance time comparison between three LWCs made with different initial thermal conductivities

be attributed to the porosity of the LWC, which makes the heat transfer inside the concrete difficult (Del Coz-Díaz 2020). The thermal conductivity of the LWC depends on the water-accessible porosity – the higher the LWC porosity, the lower the thermal conductivity (Del Coz-Díaz 2020).

When the slab is designed with a height of 120 mm of LWC, approximately four hours have to be allowed to reach the limited value of the insolation criteria (I).

For comparative reasons, LWC-2 and that of Eurocode 4 (CEN 2005) were selected. The results showed that the fire resistance time of the LWC-2 is slightly better than that of the Eurocode 4. This difference is associated with consideration, or not, of the airgap in the two materials, and can also be linked to the methodology used.

Equivalent section in fire resistance time

In this section, an attempt is made to quantify the effect of the presence of the LWC inside the composite slab with regard to the NWC at a given fire resistance class. The authors looked at finding a sufficient quantity of NWC, which may replace the quantity of the LWC in order to obtain the same fire resistance. In this study, 64 simulations were carried out on both LWC and NWC using four different composite slabs, including the re-entrant and trapezoidal profiled steel deck. Eight different slab thicknesses were selected ranging from 50 mm to 120 mm with a constant step of 10 mm. The variation parameters were regrouped in Table 4.

A calculation was performed separately on both concretes to find the necessary slab height for a given resistance time. These results are presented in Table 5.

Table 5 shows that differences in thicknesses between the two concretes (Δh_1) increase for higher fire resistance classes. For instance, the difference in the Polydeck 59S composite slabs (Δh_1) is 4 mm, 7 mm and 9 mm for R60, R90 and R120, respectively. It seems that the trapezoidal forms, namely Hi-Bond 55 and Polydeck 59S, significantly influence the value of the difference in thicknesses. This may be attributed to the fire-exposed side, which is more open than the re-entrant

Table 4 Parameters for the equivalent section study

Parameter	Concrete	
	LWC	NWC
Moisture content	3%	3%
Density (function of temp)	1 800 kg/m^3	2 300 kg/m^3
Thermal conductivity (function of temp)	1.00 W/m.K	1.95 W/m.K
Airgap	0.5 mm	0.5 mm

Table 5 Fire resistance time for each concrete LWC and NWC with different fire resistance classes

Fire resistance class	Steel deck	h_1 (mm)		Δh_1		Ac (cm^2/ml)		Δ Ac	
		LWC	NWC	(mm)	%	LWC	NWC	(cm^2)	%
R = 60 min	Cofrastar 40	56	59	3	6	862	896	34	4
	Multideck 50	51	53	2	5	913	937	24	3
	Hi-Bond 55	61	64	4	6	883	920	37	4
	Polydeck 59S	60	64	4	7	863	906	43	5
R = 90 min	Cofrastar 40	76	82	6	7	1 060	1 120	60	5
	Multideck 50	70	75	5	7	1 109	1 160	50	4
	Hi-Bond 55	80	87	6	7	1 082	1 146	64	6
	Polydeck 59S	80	87	7	8	1 060	1 128	69	6
R = 120 min	Cofrastar 40	92	100	8	8	1 225	1 307	82	6
	Multideck 50	87	94	7	8	1 274	1 346	73	5
	Hi-Bond 55	97	106	9	8	1 246	1 333	87	6
	Polydeck 59S	96	105	9	9	1 220	1 312	91	7

h_1 represents the thickness of the topping concrete
Ac represents the area of the concrete section

form. When the NWC is replaced by the LWC, the thickness of the composite slab decreases by 9% for the Polydeck 59S form at R120. This value corresponds approximately to 7% when it is estimated as a surface (Δ Ac) for 1 m length. These results have great importance when considering the cost and charges in constructing buildings.

VALIDATION OF THE MODEL WITH THE EXPERIMENTAL WORK

In order to confirm the accuracy of the model used in this study, the authors analysed certain experimental results from Del Coz-Díaz (2020) to validate their findings. The material data, such as geometrical shape, gathered from the referenced experiment, were incorporated into the numerical model for their study. The properties of these materials are regrouped in Table 6, and the results of the experimental work and the numerical model are illustrated in Figure 20.

The temperature represented by the plots was measured in points P_1 and P_2, situated at 100 mm and 40 mm from the top, respectively, as shown in Figure 20.

It is noticeable that both temperature curves for the experimental and numerical work are in the same position, the material look has similar tendencies, and they are close to each other. This demonstrates that the results of this study are reasonable and acceptable. Table 7 shows the difference between the experimental temperature readings and the temperatures predicted by the numerical model at points P1 and P2. From this it can be inferred that the numerical model is reliable and can be utilised to forecast fire resistance time for LWC.

To assess the reliability of the numerical model outcomes, the difference between the experimental and the predicted temperature by the numerical model is calculated for each point and material, as detailed in Table 7. These difference values are close to zero for several points, indicating that the method employed is acceptable.

It is worthwhile to note that the results and the deduced conclusions obtained from this study are limited to the boundary conditions (mentioned previously), geometry slabs (presented in Figure 8) and the assumed material properties (shown in Figure 5). Furthermore, only the thermal insulation criterion was applied to

Table 6 Properties of the materials used for the validation

Concrete type	Density	Moisture content	Compressive strength	Young's modulus
	kg/m³	%	MPa	MPa
LWC	1 875	4.81	25.60	$2.07 \cdot 10^4$
NWC	2 435	3.70	36.97	$4.57 \cdot 10^4$

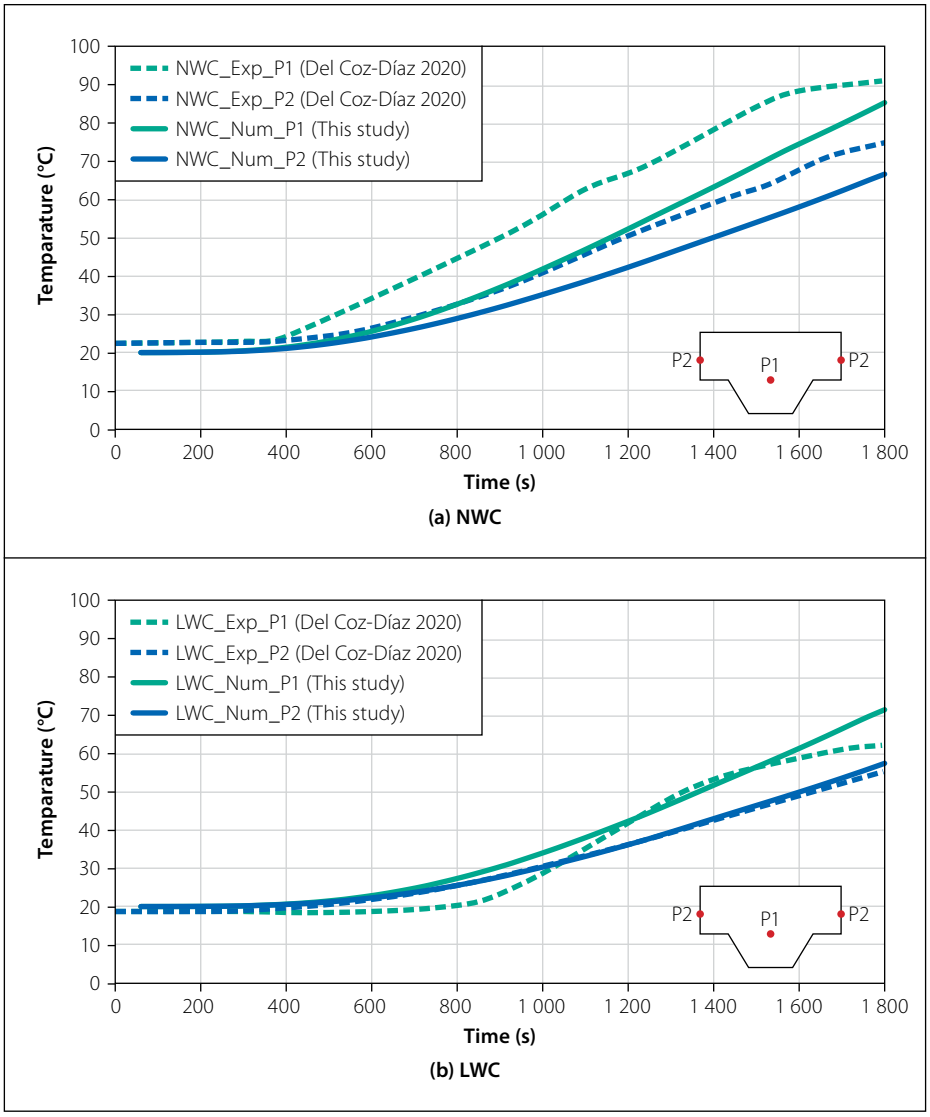


Figure 20 Temperature evolution in the different concretes

Table 7 The difference between the experimental and the predicted temperature by the numerical model

Time	Difference between EXP and NUM			
	P1 LWC	P2 LWC	P1 NWC	P2 NWC
60	1.6	1.3	2.7	2.4
300	1.7	1.4	2.2	2.3
400	2.2	1.3	2.9	2.1
600	4.1	0.6	6.9	2.3
800	7.0	0.1	10.7	3.8
1 000	4.9	0.1	15.0	6.1
1 200	0.0	0.2	14.6	8.2
1 400	1.5	0.7	14.5	9.4
1 600	2.3	1.0	13.6	8.1
1 800	9.2	2.4	5.8	8.3

determine the fire resistance time of the composite slabs. More accurate results may be found by using both the thermal insulation criterion and structural resistance in further investigations.

CONCLUSION

A numerical study was conducted to evaluate the advantages of using lightweight concrete (LWC) instead of normal-weight concrete (NWC) in composite slabs under fire conditions. The parametric analysis considered factors such as airgaps, moisture content, thermal properties of LWC, and geometric aspects. The study found that for all slab thicknesses, both maximum and average temperatures exceeded the insulation criterion limit. Finite element method (FEM) results showed that re-entrant steel decks provide greater fire resistance times compared to trapezoidal steel decks. Introducing a 1 mm airgap between the concrete and deck profile increased the fire resistance time by 15 minutes for a 100 mm thick composite slab. When moisture content exceeds 3%, the Eurocode method predicts lower fire resistance times compared to the simulation method, reducing the concrete slab density from 1 922 kg/m^3 to 1 822 kg/m^3 improved fire resistance time by approximately 12% for a 100 mm slab. To achieve the same fire resistance time, normal weight concrete sections need to be 7% thicker than lightweight concrete sections. the proposed numerical model was validated for lightweight concrete as its results closely match experimental data. The model is shown to underpredict temperatures for normal weight concrete, and merits future investigation.

REFERENCES

ANSYS n.d. ANSYS Innovation Courses. View Factors — Lesson 2. Available at: **https://innovationspace.ansys.com/courses/courses/radiation-in-heat-transfer/lessons/view-factors-lesson-2/**.

Bailey, C G 2003. Efficient arrangement of reinforcement for membrane behaviour of composite floor slabs in fire conditions. *Journal of Constructional Steel Research,* 59: 931–949. doi: 10.1016/S0143-974X(02)00116-5.

Balsa, C, Silveira, M, Mange, V & Piloto, P A G 2022. Modelling the thermal effects on structural components of composite slabs under fire conditions. *Computation (Special Issue on Applications of Computational Mathematics to Simulation and Data Analysis*), 10: 94. doi: **10.3390/computation10060094**.

Cavalline, T L, Castrodale, R W, Freeman, C & Wall, J 2017. Impact of lightweight aggregate on concrete thermal properties. *ACI Materials Journal,* 114(6). doi: **10.14359/51701003**.

CEN (European Committee for Standardization) 2002. *EN 1991-1-2: Eurocode 1: Actions on Structures. Part 1-2: General Actions. Action on Structures Exposed to Fire.* Brussels: CEN.

CEN 2005. *EN 1994-1-2: Eurocode 4: Design of Composite Steel and Concrete Structures. Part 1-2: General Rules: Structural Fire Design.* Brussels: CEN.

Davies, J M & Wang, H B 1994. Numerical temperature calculation for composite deck slabs exposed to fire. *WIT Transactions on Engineering Sciences*, Vol 5. Southampton, UK: WIT Press, pp 589–598. doi: **10.2495/HT940401**.

Del Coz-Díaz, J J, Martínez-Martínez, J E, Alonso-Martínez, M & Álvarez Rabanal, F P 2020. Comparative study of lightweight and normal concrete composite slabs behaviour under fire conditions. *Engineering Structures,* 207: 110196. doi: **10.1016/j.engstruct.2020.110196**.

Designing Buildings 2021. *Concrete-steel composite structures.* Designing Buildings, the Construction Wiki. Available at: **https://www.designingbuildings.co.uk/wiki/Concrete-steel_composite_structures**.

Fellouh, A, Bougara, A, Piloto, P A G & Benlakehal, N 2020. Non-linear buckling analysis of composite columns made from high and normal strength concrete under fire. *Asian Journal of Civil Engineering,* 21: 17–27. doi: **10.1007/s42107-019-00180-8**.

Hamerlinck, A R 1991. *The behaviour of fire-exposed composite steel/concrete slabs*. Eindhoven, Netherlands: Technische Universiteit Eindhoven. doi: **10.6100/IR348360**.

Hedjazi, S 2020. Compressive strength of lightweight concrete. In Kryvenko, P (Ed), *Compressive Strength of Concrete*. IntechOpen. doi: **10.5772/intechopen.88057**.

Huang, Z, Burgess, I W & Plank, R J 2004. Fire resistance of composite floors subject to compartment fires. *Journal of Constructional Steel Research,* 60: 339–360. doi: **10.1016/j.jcsr.2003.08.012**.

Jiang, J, Main, J A, Sadek, F H & Weigand, J M 2017. *Numerical modeling and analysis of heat transfer in composite slabs with profiled steel decking.* Report No. NIST TN 1958. Gaithersburg, MD: US National Institute of Standards and Technology. doi: **10.6028/NIST.TN.1958**.

Jiang, J, Pintar, A, Weigand, J M, Main, J A & Sadek, F 2019. Improved calculation method for insulation-based fire resistance of composite slabs. *Fire Safety Journal,* 105: 144–153. doi: **10.1016/j.firesaf.2019.02.013**.

Lawson, R M 2006. *Dalles mixtes pour bâtiments multi-étagés destinés à un usage commercial et résidentiel*. Available at: **https://www.cticm.com/centre-de-ressources/?fwp_taxonomy_first_line=librairie-documentation&fwp_taxonomy_second_line=doc-projet&fwp_projet=access-steel&fwp_category_projet=phase-avant-projet#woo-login-popup-sc-login**.

Li, G-Q, Zhang, N & Jiang, J 2017. Experimental investigation on thermal and mechanical behaviour of composite floors exposed to standard fire. *Fire Safety Journal,* 89: 63–76. doi: **10.1016/j.firesaf.2017.02.009**.

Piloto, P A, Prates, L M & Rigobello, R G 2018. Numerical simulation of the fire resistance of composite slabs with steel deck. *International Journal of Engineering and Technology (UAE),* 7: 83–86. doi: **10.14419/ijet.v7i2.23.11889**.

Piloto, P A G, Balsa, C, Ribeiro, F & Rigobello, R 2021. Computational simulation of the thermal effects on composite slabs under fire conditions. *Journal of Mathematics and Computer Science*, 15: 155–171. doi: **10.1007/s11786-020-00466-0**.

Punlert, S, Laoratanakul, P, Kongdee, R & Suntako, R 2017. Effect of lightweight aggregates prepared from fly ash on lightweight concrete performances. *Journal of Physics: Conference Series*, 901: 012086. doi: **10.1088/1742-6596/901/1/012086**.

Rackham, J W, Couchman, G H & Hicks, S J 2009. *Composite slabs and beams using steel decking: Best practice for design and construction* (Revised ed.) MCRMA Technical Paper. Wirral, Cheshire, UK: Metal Cladding & Roofing Manufacturers Association in partnership with the Steel Construction Institute.

Shah, J U & Vadik, M D 2004. Parametric study of composite slab using finite element analysis. *International Journal of Futuristic Trends in Engineering and Technology*, 1(3).

Wickström, U 2016. *Temperature Calculation in Fire Safety Engineering.* Cham, Switzerland: Springer International. doi: **10.1007/978-3-319-30172-3**.

Zhao, H, Zhao, J, Wang, R, Zhang, W, Liu, F & Wu, S 2022. Thermal behaviour of composite slabs with closed profiled steel decking and recycled aggregate concrete in fire. *Fire Safety Journal,* 132: 103637. doi: **10.1016/j.firesaf.2022.103637**.